

# Biodistribution and photodynamic effects of polyvinylpyrrolidone-hypericin using multicellular spheroids composed of normal human urothelial and T24 transitional cell carcinoma cells

Joachim Vandepitte,<sup>a</sup> Mieke Roelants,<sup>a</sup> Ben Van Cleynenbreugel,<sup>b</sup> Klaudia Hettinger,<sup>c</sup> Evelyne Lerut,<sup>d</sup> Hendrik Van Poppel,<sup>b</sup> and Peter A. M. de Witte<sup>a</sup>

<sup>a</sup>Katholieke Universiteit Leuven, Faculteit Farmaceutische Wetenschappen, Laboratorium voor Farmaceutische Biologie, B-3000 Leuven, Belgium

<sup>b</sup>Katholieke Universiteit Leuven, Faculteit Geneeskunde, Dienst Urologie, B-3000 Leuven, Belgium

<sup>c</sup>Sanochemia Pharmazeutika AG, 1090 Vienna, Austria

<sup>d</sup>Katholieke Universiteit Leuven, Faculteit Geneeskunde, Afdeling Cellulaire Morfologie en Pathologie, B-3000 Leuven, Belgium

**Abstract.** Polyvinylpyrrolidone (PVP)-hypericin is a potent photosensitizer that is used in the urological clinic to photodiagnose with high-sensitivity nonmuscle invasive bladder cancer (NMIBC). We examined the differential accumulation and therapeutic effects of PVP-hypericin using spheroids composed of a human urothelial cell carcinoma cell line (T24) and normal human urothelial (NHU) cells. The *in vitro* biodistribution was assessed using fluorescence image analysis of 5- $\mu\text{m}$  cryostat sections of spheroids that were incubated with PVP-hypericin. The results show that PVP-hypericin accumulated to a much higher extent in T24 spheroids as compared to NHU spheroids, thereby reproducing the clinical situation. Subsequently, spheroids were exposed to different PDT regimes with a light dose ranging from 0.3 to 18 J/cm<sup>2</sup>. When using low fluence rates, only minor differences in cell survival were seen between normal and malignant spheroids. High light fluence rates induced a substantial difference in cell survival between the two spheroid types, killing ~80% of the cells present in the T24 spheroids. It was concluded that further *in vivo* experiments are required to fully evaluate the potential of PVP-hypericin as a phototherapeutic for NMIBC, focusing on the combination of the compound with methods that enhance the oxygenation of the urothelium. © 2011 Society of Photo-Optical Instrumentation Engineers (SPIE). [DOI: 10.1117/1.3533316]

Keywords: bladder cancer; PVP-hypericin; biodistribution; photodynamic therapy; tumor spheroids.

Paper 10395R received Jul. 12, 2010; revised manuscript received Nov. 17, 2010; accepted for publication Nov. 18, 2010; published online Jan. 27, 2011.

## 1 Introduction

In 2008, bladder cancer was the sixth most diagnosed malignancy in Europe, occurring three to four times more in men than in women.<sup>1</sup> This disease, with a heterogeneous manifestation, ranges from low-grade Ta tumors with a good prognosis to high-grade carcinomas with a high mortality rate. Today, treatment of nonmuscle invasive bladder cancer (NMIBC) is mainly based on transurethral resection of the bladder (TURB) followed by intravesical instillation of mitomycin-C or bacillus Calmette-Guérin (BCG).<sup>2</sup> However, because NMIBC is mostly multifocal and not readily visible and because the lumen of the bladder is easily accessible by endoscopy, superficial bladder cancer lesions are ideally suited to treatment with photodynamic therapy (PDT).<sup>3,4</sup> This treatment modality involves the administration of a photosensitizer (or a precursor), which is specifically retained by or accumulates to a higher extent in tumor cells.<sup>5</sup> Subsequent illumination with light of an appropriate wavelength excites the photosensitizer, eventually causing tumor damage via photosensitization reactions.

The safety of whole-bladder PDT critically depends on the selective uptake of the photoactive drug by the malignant tissue to avoid major side effects, such as fibrosis and contraction of the bladder.<sup>6</sup> Recently, aminolevulinic acid (ALA) has successfully been applied in the treatment of recurrent superficial bladder cancer without persistent reduction in bladder capacity.<sup>7-9</sup> ALA is a precursor in the biosynthesis of heme and induces the production of the endogenous photosensitizer protoporphyrin IX (PpIX). Because this process of biochemical conversion occurs up to 10 times more in tumor than normal tissue, ALA-induced PpIX can safely be used in whole-bladder PDT.<sup>10</sup>

Hypericin is another potent photosensitizer that accumulates with high sensitivity and specificity in NMIBC lesions after intrabladder instillation.<sup>11-13</sup> The mechanism underlying the tumor-tropic characteristics of the selectivity is not fully understood. It is assumed that the enhanced uptake of hypericin is secondary to a loss of intercellular adhesion in malignant tissue (e.g., by a decreased expression of E-cadherin in cancer cells<sup>14,15</sup>), resulting in an enhanced intralesional migration of the compound by a paracellular route.

In water, hypericin forms macroaggregates, hereby losing its spectroscopic and tumor-selective properties.<sup>16</sup> In

Address all correspondence to: Peter A. M. de Witt, Laboratorium voor Farmaceutische Biologie, Faculteit Farmaceutische Wetenschappen, Katholieke Universiteit Leuven, Herestraat 49, bus 824, B-3000 Leuven, Belgium. Tel: 32-16-323432; Fax: 32-16-323460; E-mail: peter.dewitte@pharm.kuleuven.be.

previous clinical studies, this problem was overcome by using hypericin formulations supplemented with 1% plasma proteins.<sup>11,12</sup> More recently, an alternative formulation was developed based on polyvinylpyrrolidone (PVP) that complexes with hypericin and renders the molecule water soluble.<sup>17</sup> This specific formulation of hypericin appeared to be also very suitable for the fluorescence detection of NMIBC.<sup>18</sup>

In this paper, we describe the differential accumulation and therapeutic effects of PVP-hypericin in spheroids composed of a human urothelial cell carcinoma cell line (T24) and NHU cells. Spheroids are 3-D multicellular clusters that share important features with small avascular tumors, such as their histoarchitecture, their gradients of nutrients, oxygen levels, proliferation rate, and pH.<sup>19</sup> Hence, they are an excellent model to assess the PDT effects on NMIBC lesions in a preclinical setting.

Our results show that PVP-hypericin accumulated to a much higher extent in T24 spheroids as compared to NHU spheroids, thereby reflecting the clinical situation in which PVP-hypericin accumulates preferentially in the malignant urothelium.<sup>18</sup> High light fluence rates induced a substantial difference in cell survival between the two spheroid types, killing ~80% of the cells present in the T24 spheroids.

## 2 Materials and Methods

### 2.1 Tumor Cell Lines

T24 [transitional cell carcinoma (TCC), urinary bladder, human] was obtained from American Type Culture Collection (ATCC, Rockville, Maryland). Cells were cultured in 175-cm<sup>2</sup> tissue culture flasks at 37°C in a humidified atmosphere containing 5% CO<sub>2</sub> and 95% air in minimum essential medium (MEM) with Earle's salts containing 2 mM L-glutamine, 1% antibiotic/antimycotic solution, 1% nonessential amino acids, tylosine (60 µg/ml) (Eli Lilly, Brussels, Belgium), and 10% fetal calf serum (FCS). All culture medium compounds were purchased from Invitrogen (Merelbeke, Belgium).

### 2.2 NHU Cells

NHU cells were obtained from the ureter of multiple patients undergoing nephrectomy, following standard departmental procedures. The histology confirmed benign urothelium in each case. Specimens were dissected, and NHU cells were isolated and cultured as reported previously.<sup>20</sup> Cells were cultured in 250 ml primary flasks (Becton Dickinson, Mylan cedex, France) in keratinocyte serum-free medium (KSFM) supplemented with 5 ng/ml epidermal growth factor, 50 µg/ml bovine pituitary extract (Gibco-BRL, Paisley, Scotland), and 30 ng/ml cholera toxin (Sigma, Bornem, Belgium). Cultures were maintained at 37°C in a humidified atmosphere of 5% CO<sub>2</sub> and 95% air. Cells were passaged when near or just confluent by incubating the cell monolayer with 0.2 ml/cm<sup>2</sup> phosphate buffered saline (PBS) containing 0.1% ethylenediaminetetraacetic acid (EDTA) (Acros, Geel, Belgium) for 5 min at 37°C. The solution was replaced with 0.25% trypsin/0.02% EDTA (Sigma) in Hanks balanced salt solution (without Ca<sup>2+</sup> or Mg<sup>2+</sup>) until the cells detached. Soybean trypsin inhibitor (Sigma) was then added (2.5 mg/ml trypsin-EDTA solution). After centrifugation at 250 g for 4 min, cells were seeded at a ratio of 1:3 to 1:6. For all experiments, cells were used from culture passages 4–6.

### 2.3 3-D Cell Culture

Both tumor and NHU spheroids were prepared using the liquid overlay technique.<sup>21</sup> Cell culture 96-well plates were underlaid with 1.5% agarose (Sigma-Aldrich) in MEM. Spheroids were initiated in MEM for TCC cells and in KSFM for NHU cells, by plating 5 × 10<sup>3</sup> cells (per well) in 200 µl of growth medium containing 1% of sodium pyruvate (Invitrogen, Merelbeke, Belgium). The medium was replaced once during the growth of the spheroids. All experiments were performed on spheroids with an average diameter of 300 µm.

### 2.4 Fluorescence Distribution in Spheroids and Quantification

Spheroids were incubated with a freshly prepared PVP-hypericin solution (10 and 30 µM in 0.9% NaCl in the absence of FCS) for 2 h. Afterward they were washed twice with PBS, transferred into TissueTek embedding medium (Miles, Elkhart, Indiana), and snap frozen in liquid nitrogen. Then, 5-µm cryostat sections of the spheroids were made, and imaging of fluorescence was achieved using fluorescence microscopy. The fluorescence microscope consisted of an Axioskop 2 plus fluorescence microscope (Carl Zeiss, Vision, Göttingen, Germany) illuminated by a 100-W mercury lamp. For fluorescence imaging of PVP-hypericin, the filter set used consisted out of a 510- to 560-nm bandpass excitation filter and a 590-nm long-pass emission filter. Fluorescence images were taken using a light-sensitive charge-coupled device digital camera (AxioCam HR, Carl Zeiss, Göttingen, Germany). To assess and quantify the fluorescence present in centrally cut spheroid sections, a KS imaging software system (Carl Zeiss, Hallbergmoos, Germany) was used. Fluorescence was measured in concentric layers of 1.9 µm from the rim (F<sub>max</sub>) to the center (F<sub>min</sub>) of the spheroid and corrections were made for autofluorescence. Fluorescence was determined as the mean of six spheroids.

### 2.5 In Vitro PDT

Both T24 and NHU spheroids were incubated with a freshly prepared 30 µM PVP-hypericin solution for 2 h. After the incubation, spheroids were washed with PBS, transferred into a 24-well plate (10 spheroids/well) containing 0.5 ml PBS, and were light treated. The light irradiation was carried out using light emitted by a rhodamine 6G dye laser (375B, Spectra-Physics, Mountain View, California) pumped by a 4-W argon-laser (Spectra-Physics, Mountain View, California). The laser is coupled into a fiberoptic microlens (Rare Earth Medical, West Yarmouth, Massachusetts) to obtain an ultrauniform intensity distribution. The laser was tuned at 595 nm, and the laser beam directed to six wells containing the spheroids (three wells with PVP-hypericin and three wells without PVP-hypericin). The latter was set as the control group (100% survival). The fluence rates used were 1 and 5 mW/cm<sup>2</sup>, and the irradiation times were 5, 15, and 60 min. Therefore, the total fluence ranged from 0.3 to 18 J/cm<sup>2</sup>.

After light treatment, PBS was replaced by fresh supplemented MEM or KSFM in case of T24 and NHU spheroids, respectively, and 24-h later, cell proliferation was determined by the use of the 3-(4,5-dimethylthiazol-2-yl)-2,5-diphenyl-tetrazolium bromide [(MTT), Sigma, St. Louis, Missouri]

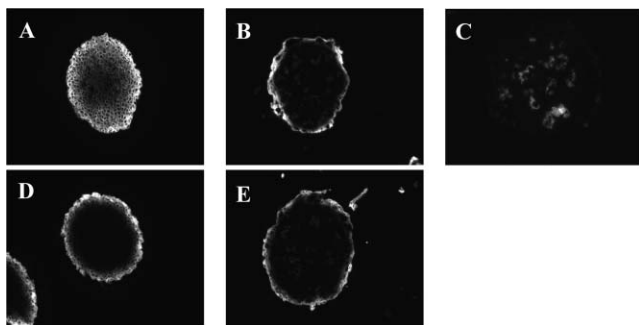


**Fig. 1** Typical fluorescence photomicrographs of (a, d) 5- $\mu\text{m}$  cryostat sections of T24 and (b, c, e) NHU spheroids incubated with (a, b) 30  $\mu\text{M}$  and (d, e) 10  $\mu\text{M}$  PVP-hypericin. Note the presence of the fluorescent inclusion bodies present in control NHU spheroids (no PVP-hypericin) (c). Different gain settings have been used: (a, d) = Gain 1; (b, e) = Gain 2; (c) = Gain 3. Gain 1–4 denotes the gain at which the fluorescence was measured (e.g., Gain 4 = highest sensitivity, Gain 1 = lowest sensitivity). Original magnification = 200X.

dye-reduction assay. MTT was dissolved in medium and added to the cells (3 mg/ml, 0.5 ml), and the plates were incubated at 37°C for  $\sim$ 4 h. Before solubilizing the formed formazan crystals in isopropanol, T24 spheroids were left in 0.05% trypsin for 30 min. The control group consisted of spheroids that were irradiated without PVP-hypericin. After solubilizing the formazan crystals in isopropanol, the solution was transferred in 96-well plates that were read by a microtiter plate reader (SLT, Salzburg, Austria) at 550 nm. All experiments were performed in triplicate.

### 3 Results

#### 3.1 Biodistribution of PVP-hypericin

The *in vitro* biodistribution of PVP-hypericin was compared in spheroids derived from normal human urothelial (NHU) cells and T24 bladder cancer cells, using fluorescence microscopical analysis of cryostat sections.

Figure 1 shows typical fluorescence photomicrographs of 5- $\mu\text{m}$  spheroid sections that were incubated with 10 or 30  $\mu\text{M}$  PVP-hypericin. T24 spheroids, incubated with 30  $\mu\text{M}$

PVP-hypericin exhibited a high fluorescence at the rim that slowly declined toward the center of the spheroid [Fig. 1(a)]. When a concentration of 10  $\mu\text{M}$  PVP-hypericin was used, fluorescence values were substantially lower at the surface and virtually no fluorescence was observed in the inner parts of the spheroids [Fig. 1(d)]. The fluorescence present in NHU spheroids incubated with either of the concentrations of PVP-hypericin was also restricted mainly to the outer rim of the spheroid [Figs. 1(b) and 1(e)]. In the case of NHU spheroids, some fluorescent inclusions in control spheroids (no PVP-hypericin) were found of unknown origin and composition [Fig. 1(c)].

Consequently, fluorescence was quantified using imaging software (Table 1 and Fig. 2). Table 1 shows the mean of the maximum and the minimum fluorescence as well as the mean fluorescence at a distance of 25  $\mu\text{m}$  ( $F_{25}$ ) and 50  $\mu\text{m}$  ( $F_{50}$ ) from the rim of the spheroid. The differential accumulation of PVP-hypericin in NHU spheroids or T24 spheroids is best seen at a concentration of 30  $\mu\text{M}$ . The ratio of fluorescence present in T24 and NHU spheroids is 19 and 80 at a distance of 25 and 50  $\mu\text{m}$ , respectively, whereas the ratio is only 3 and 2 at the same distance using 10  $\mu\text{M}$  PVP-hypericin. These results very clearly demonstrate lack of penetration of PVP-hypericin into NHU spheroids.

#### 3.2 PDT Effects of PVP-Hypericin

Photodynamic treatment of NHU and T24 spheroids was performed after incubation with 30  $\mu\text{M}$  PVP-hypericin for 2 h, and 24 h after light irradiation, we assessed the relative survival of both NHU and T24 spheroids in similar light conditions by MTT assay (Fig. 3). When using a fluence rate of 1 mW/cm<sup>2</sup>, the total light dose amounted between 0.3 and 3.6 J/cm<sup>2</sup> [Fig. 3(a)]. A significant difference in survival between the two spheroid types was seen only with an irradiation time of 15 min. Survival rates in NHU spheroids remained above 80% after short light irradiations but dropped in the case of a 60-min irradiation (i.e., 47.7  $\pm$  23.7%). In T24 spheroids, there was a gradual decrease in survival rate as a function of the irradiation time. When spheroids

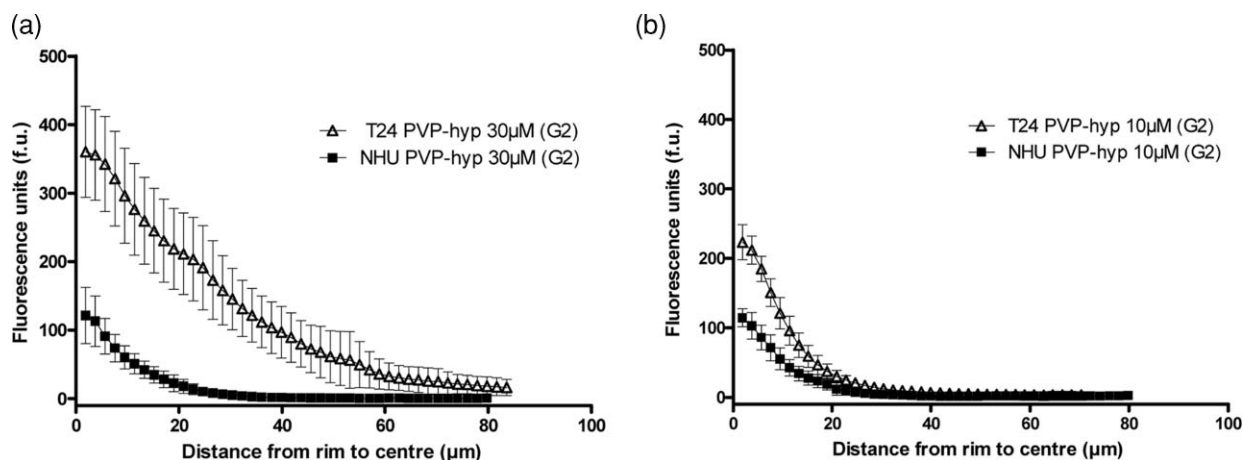


**Fig. 2** Quantification of the fluorescence measured in spheroids after incubation with (a) 30  $\mu\text{M}$  and (b) 10  $\mu\text{M}$  PVP-hypericin. Fluorescence was measured in concentric layers of 1.9- $\mu\text{m}$  thickness in T24 (open triangles) and NHU (closed squares) spheroid sections. Each value represent the mean  $\pm$  SD ( $n = 6$ ). All measurements were made using a gain setting of 2.

**Table 1** Fluorescence values measured at the rim ( $F_{\max}$ ) of the spheroid, at 25  $\mu\text{m}$  ( $F_{25}$ ), at 50  $\mu\text{m}$  ( $F_{50}$ ), and at the center of the spheroid ( $F_{\min}$ ).

	30 $\mu\text{M}$ PVP hypericin			
	$F_{\max} \pm \text{SD}$	$F_{25} \pm \text{SD}$	$F_{50} \pm \text{SD}$	$F_{\min} \pm \text{SD}$
	***	***	**	**
T24	360 $\pm$ 66.5	191 $\pm$ 37.8	61,4 $\pm$ 37.8	16,4 $\pm$ 11.8
NHU	121 $\pm$ 41.0	10,4 $\pm$ 6.20	0,77 $\pm$ 0.59	0,74 $\pm$ 0.44
	10 $\mu\text{M}$ PVP hypericin			
	***	**	*	*
T24	223 $\pm$ 25.1	20.4 $\pm$ 6.10	4.65 $\pm$ 1.30	3.5 $\pm$ 1.40
NHU	114 $\pm$ 13.1	7.34 $\pm$ 5.19	2.60 $\pm$ 1.71	1.50 $\pm$ 1.09

Spheroids were incubated with 10 or 30  $\mu\text{M}$  PVP-hypericin for 2 h. Frozen section were analyzed with fluorescence microscopy and image analysis software. Fluorescence values of T24 spheroids were compared to fluorescence values of NHU spheroids at the same distance towards the rim of the spheroid. Data represent the mean  $\pm$  SD ( $n=6$ ) ns=not significant; \* $p < 0.05$ ; \*\* $p < 0.01$ ; \*\*\* $p < 0.001$ .

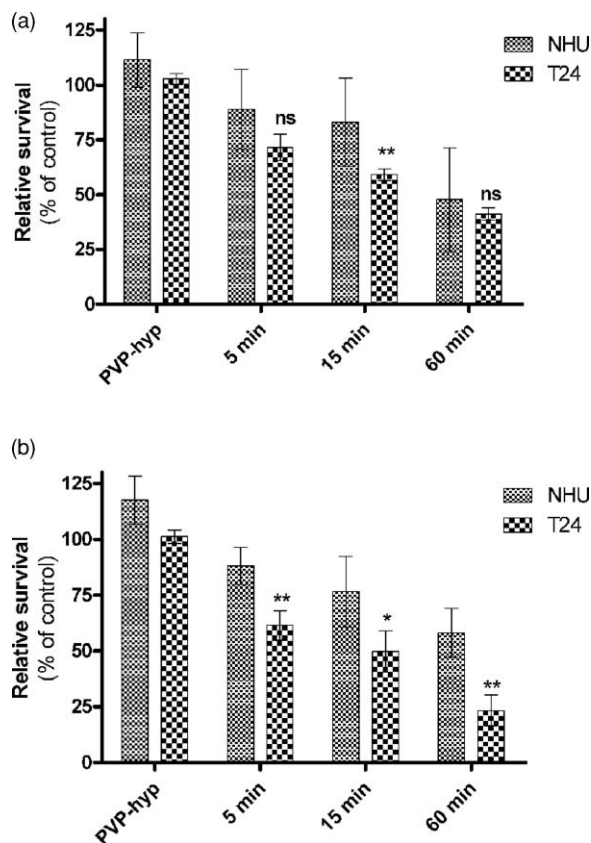


**Fig. 3** Relative survival of NHU vs T24 cells after exposure of spheroids to 30  $\mu\text{M}$  PVP-hypericin and different light conditions (a) 1  $\text{mW}/\text{cm}^2$  (b) 5  $\text{mW}/\text{cm}^2$  for 5, 15, or 60 min. PVP-hyp: conditions without light. Control spheroids were treated with light only, and cell survival was set as 100%. All values are presented as mean  $\pm$  SD; \*  $p < 0.05$ ; \*\*  $p < 0.01$ .

were irradiated with a fluence rate of 5  $\text{mW}/\text{cm}^2$ , on the other hand, there was a significant difference in survival rates between the NHU and T24 spheroids at all irradiation times [Fig. 3(b)]. In these conditions, the total light fluence ranged from 1.5 to 18  $\text{J}/\text{cm}^2$ . With increasing irradiation times, there was a general decrease in survival rates in both spheroid types, albeit more pronounced in T24 spheroids.

The administration of PVP-hypericin alone (Fig. 3) or light alone (results not shown) did not cause any change in survival rate of cells present in either of the spheroids.

## 4 Discussion

We first investigated the biodistribution of PVP-hypericin in a 3-D spheroid system consisting of T24 bladder cancer tumor cells or NHU cells. When using 10  $\mu\text{M}$  PVP-hypericin, a somewhat similar limitedly differential uptake between normal and malignant spheroids was observed in this study as compared to previously published results using 10  $\mu\text{M}$  hypericin 14. However, when using 30  $\mu\text{M}$  PVP-hypericin, the present results showed a dramatically increased difference between the uptake of the compound in both types of spheroids.

Of interest, in the previous study hypericin was solubilized in the incubation medium using FCS, whereas in this study hypericin is complex and consequently made water-soluble with PVP. The data therefore seem to indicate that the mechanism underlying the specific penetration of hypericin in malignant tissue is unrelated to the specific formulation that is used. It is mainly the appropriate affinity of hypericin for specific carriers and cellular membranes that are key to the selective intracellular accumulation in malignant tissue. When hypericin is bound to constituents of FCS (e.g., using lipoproteins (LDL, HDL) or complexed to PVP, passive paracellular transport can take

place and depending on the avidity of hypericin to its carriers, hypericin is taken up intracellularly.

Our study further indicates that the uptake of PVP-hypericin in malignant spheroids is in close agreement with the outcome of a study where fluorescence cystoscopy with PVP-hypericin was performed on patients with suspected primary or recurrent bladder malignancies. It was found that the sensitivity in the diagnosis of carcinoma *in situ* (CIS) was 100% compared to 33% for whole light endoscopy,<sup>18</sup> suggesting a high accumulation of PVP-hypericin in these lesions. Of interest, CIS is a small malignant tumor with a nonvascularized histoarchitecture that resembles well the histological background of spheroids.

On the other hand, in the urological clinic, bladders were instilled with 10  $\mu\text{M}$  PVP-hypericin,<sup>18</sup> a concentration which in this study, and contrary to the outcome with 30  $\mu\text{M}$  PVP-hypericin, resulted in a limitedly differential uptake of PVP-hypericin in normal versus malignant spheroids. In this context, however, it should be noted that cystoscopy is typically used in the clinic as a technique to collect diagnostic information from the bladder surface. For that purpose, the tube of the cystoscope is positioned at the surface of the bladder urothelium, which is perpendicular to the viewing direction of the fluorescence microscope that visualizes the fluorescence present in transected spheroids. Unfortunately, it is presently unknown to what extent this difference affects the outcome of the fluorescence measurements in the preclinical versus the clinical situation.

The specific accumulation in malignant tissue combined with its photosensitizing properties makes PVP-hypericin a very promising tool for the photodynamic treatment of NMIBC. To characterize the photodependent antitumoral properties of PVP-hypericin, we studied PDT-induced cell death in the normal and malignant spheroids. To that end, spheroids were preincubated with 30  $\mu\text{M}$  PVP-hypericin, a concentration that resulted in a maximal differential uptake of the compound in both types of spheroids. The results show that by using the currently used fluence rates and irradiation times, we were not capable of inducing 100% cell death. Significantly, in a previous study it was noted that hypericin-incubated spheroids that were dissociated prior to light irradiation, were approximately 2000-fold more sensitive than the intact spheroids, and as sensitive as monolayer cells exposed to hypericin PDT.<sup>22</sup> In these monolayer conditions, oxygen depletion can be ruled out during PDT. Hence, despite the low fluence rates used (i.e., 1 and 5  $\text{mW}/\text{cm}^2$ ), the incomplete response seen in this study is likely due to a fast PDT-dependent consumption of oxygen, which is not counteracted by an adequate intraspheroidal diffusion of oxygen from the immediate aqueous surrounding. The limited differential response of the normal and malignant spheroids can also be accounted for by a similar mechanism. Indeed, despite the dramatic difference in photosensitizer content of both types of spheroids, it is believed that the excess of PVP-hypericin in the malignant spheroids, due to a shortage of oxygen, does not result in a large additional photodynamic effect.

Because the presence and diffusion of oxygen in tissue that is treated are crucial to the outcome, one has to look for opportunities to enhance the oxygenation state of the biological PDT target. Thus far, two methods were tested with great success and dramatically increased the PDT effects in conditions similar to the ones used in this study. One technique used normobaric oxygen that was simply bubbled through the solution

that surrounded the spheroids, whereas the other approach used a biocompatible perfluorocarbon as oxygen carrier to hyperoxygenate the biological surrounding.<sup>23,24</sup> Because both modalities are rather easy to apply to the bladder cavity, PDT with PVP-hypericin combined with either of the techniques looks very promising for an efficient and selective whole-bladder-wall photodynamic antitumoral treatment in a urological clinical setting. Obviously, further *in vivo* experiments are required to fully evaluate the potential of PVP-hypericin as a phototherapeutic, focusing on the combination of the compound with methods that enhance the oxygenation of the urothelium.

### Acknowledgments

This work was supported by grants awarded by “Fonds voor Wetenschappelijk Onderzoek-Vlaanderen (F.W.O.-Vlaanderen) and by the K.U.Leuven (onderzoekstoelage) and Sanochemia Pharmazeutika AG (Austria).

### References

1. J. Ferlay, D. M. Parkin, and E. Steliarova-Foucher, “Estimates of cancer incidence and mortality in Europe in 2008,” *Eur. J. Cancer* **46**(4), 765–781 (2010).
2. K. Hendricksen and J. A. Witjes, “Current strategies for first and second line intravesical therapy for nonmuscle invasive bladder cancer,” *Curr. Opin. Urol.* **17**(5), 352–357 (2007).
3. P. Jichlinski and H. J. Leisinger, “Photodynamic therapy in superficial bladder cancer: past, present and future,” *Urol. Res.* **29**(6), 396–405 (2001).
4. D. C. Shackley, C. Whitehurst, J. V. Moore, N. J. George, C. D. Betts, and N. W. Clarke, “Light penetration in bladder tissue: implications for the intravesical photodynamic therapy of bladder tumours,” *BJU Int.* **86**(6), 638–643 (2000).
5. D. E. Dolmans, D. Fukumura, and R. K. Jain, “Photodynamic therapy for cancer,” *Nat. Rev. Cancer* **3**(5), 380–387 (2003).
6. M. Triesscheijn, P. Baas, J. H. Schellens, and F. A. Stewart, “Photodynamic therapy in oncology,” *Oncologist* **11**(9), 1034–1044 (2006).
7. R. Waidelich, W. Beyer, R. Knuchel, H. Stepp, R. Baumgartner, J. Schroder, A. Hofstetter, and M. Kriegmair, “Whole bladder photodynamic therapy with 5-aminolevulinic acid using a white light source,” *Urology* **61**(2), 332–337 (2003).
8. M. Kriegmair, R. Baumgartner, W. Lumper, R. Waidelich, and A. Hofstetter, “Early clinical experience with 5-aminolevulinic acid for the photodynamic therapy of superficial bladder cancer,” *Br. J. Urol.* **77**(5), 667–671 (1996).
9. R. J. Skyrme, A. J. French, S. N. Datta, R. Allman, M. D. Mason, and P. N. Matthews, “A phase-1 study of sequential mitomycin C and 5-aminolevulinic acid-mediated photodynamic therapy in recurrent superficial bladder carcinoma,” *BJU Int.* **95**(9), 1206–1210 (2005).
10. S. Collaud, A. Juzeniene, J. Moan, and N. Lange, “On the selectivity of 5-aminolevulinic acid-induced protoporphyrin IX formation,” *Curr. Med. Chem. Anticancer Agents* **4**(3), 301–316 (2004).
11. M. A. D’Hallewin, P. A. De Witte, E. Waelkens, W. Merlevede, and L. Baert, “Fluorescence detection of flat bladder carcinoma *in situ* after intravesical instillation of hypericin,” *J. Urol.* **164**(2), 349–351 (2000).
12. M. A. D’Hallewin, A. R. Kamuhabwa, T. Roskams, P. A. De Witte, and L. Baert, “Hypericin-based fluorescence diagnosis of bladder carcinoma,” *BJU Int.* **89**(7), 760–763 (2002).
13. H. G. Sim, W. K. Lau, M. Olivo, P. H. Tan, and C. W. Cheng, “Is photodynamic diagnosis using hypericin better than white-light cystoscopy for detecting superficial bladder carcinoma?” *BJU Int.* **95**(9), 1215–1218 (2005).
14. A. Huygens, A. R. Kamuhabwa, T. Roskams, B. Van Cleynenbreugel, H. Van Poppel, and P. A. de Witte, “Permeation of hypericin in spheroids composed of different grade transitional cell carcinoma cell lines and normal human urothelial cells,” *J. Urol.* **174**(1), 69–72 (2005).

15. A. Huygens, I. Crnolatac, J. Develter, B. Van Cleynenbreugel, T. Van der Kwast, and P. A. de Witte, "Differential accumulation of hypericin in spheroids composed of T-24 transitional cell carcinoma cells expressing different levels of E-cadherin," *J. Urol.* **179**(5), 2014–2019 (2008).
16. M. Van De Putte, T. Roskams, G. Bormans, A. Verbruggen, and P. A. De Witte, "The impact of aggregation on the biodistribution of hypericin," *Int. J. Oncol.* **28**(3), 655–660 (2006).
17. A. Kubin, H. G. Loew, U. Burner, G. Jessner, H. Kolbabeck, and F. Wierrani, "How to make hypericin water-soluble," *Pharmazie* **63**(4), 263–269 (2008).
18. A. Kubin, P. Meissner, F. Wierrani, U. Burner, A. Bodenteich, A. Pytel, and N. Schmeller, "Fluorescence diagnosis of bladder cancer with new water soluble hypericin bound to polyvinylpyrrolidone: PVP-hypericin," *Photochem. Photobiol.* **84**(6), 1560–1563 (2008).
19. S. J. Madsen, C. H. Sun, B. J. Tromberg, V. Cristini, N. De Magalhaes, and H. Hirschberg, "Multicell tumor spheroids in photodynamic therapy," *Lasers Surg. Med.* **38**(5), 555–564 (2006).
20. J. Southgate, K. A. Hutton, D. F. Thomas, and L. K. Trejdosiewicz, "Normal human urothelial cells in vitro: proliferation and induction of stratification," *Lab. Invest.* **71**(4), 583–594 (1994).
21. J. M. Yuhas, A. P. Li, A. O. Martinez, and A. J. Ladman, "A simplified method for production and growth of multicellular tumor spheroids," *Cancer Res.* **37**(10), 3639–3643 (1977).
22. A. R. Kamuhabwa, A. Huygens, and P. A. De Witte, "Photodynamic therapy of transitional cell carcinoma multicellular tumor spheroids with hypericin," *Int. J. Oncol.* **23**(5), 1445–1450 (2003).
23. A. R. Kamuhabwa, A. Huygens, T. Roskams, and P. A. De Witte, "Enhancing the photodynamic effect of hypericin in human bladder transitional cell carcinoma spheroids by the use of the oxygen carrier, perfluorodecalin," *Int. J. Oncol.* **28**(3), 775–780 (2006).
24. A. Huygens, A. R. Kamuhabwa, A. Van Laethem, T. Roskams, B. Van Cleynenbreugel, H. Van Poppel, P. Agostinis, and P. A. De Witte, "Enhancing the photodynamic effect of hypericin in tumour spheroids by fractionated light delivery in combination with hyperoxygenation," *Int. J. Oncol.* **26**(6), 1691–1697 (2005).